

Evolution of N defect states and optical transitions in ordered and disordered $\text{GaP}_{1-x}\text{N}_x$ alloys

This article has been downloaded from IOPscience. Please scroll down to see the full text article.

2008 J. Phys.: Condens. Matter 20 295211

(<http://iopscience.iop.org/0953-8984/20/29/295211>)

View [the table of contents for this issue](#), or go to the [journal homepage](#) for more

Download details:

IP Address: 129.252.86.83

The article was downloaded on 29/05/2010 at 13:35

Please note that [terms and conditions apply](#).

Evolution of N defect states and optical transitions in ordered and disordered GaP_{1-x}N_x alloys

C Harris¹, A Lindsay¹ and E P O'Reilly^{1,2}

¹ Tyndall National Institute, Lee Maltings, Cork, Republic of Ireland

² Department of Physics, University College Cork, Republic of Ireland

Received 16 May 2008

Published 26 June 2008

Online at stacks.iop.org/JPhysCM/20/295211

Abstract

We show using an sp^3s^* tight-binding model that the band anti-crossing (BAC) model describes well the evolution of the lowest N-related conduction states in ordered GaP_{1-x}N_x alloys, including the evolution of the Γ character with increasing x . We obtain a good description of the lowest conduction states in disordered GaPN structures by explicitly treating the interaction between the GaP host Γ conduction band minimum and defect states associated with a random distribution of N atoms. We find a very similar value for the total Γ character mixed into the N levels in the ordered and disordered cases, but a wider distribution of states with Γ character in the disordered case. We show that the band gap reduction with increasing composition is dominated by the increasing formation of N cluster states. Overall key features of the band structure can be well described using a modified BAC model which explicitly includes the broad distribution of N levels in disordered GaPN alloys.

1. Introduction

At present there is controversy as to the nature of the lowest conduction states and of the band gap for dilute GaP_{1-x}N_x alloys. Replacing a small fraction of phosphorus by nitrogen in GaP_{1-x}N_x produces states in the band gap close to and just below the host GaP X point conduction band minimum energy. The main models in the literature to describe the evolution of these states are an impurity-band (IB) model [1, 2], an empirical pseudopotential-based model [3–5], and a two-level band anti-crossing (BAC) model [6–10]. In the IB model the N-induced states broaden with increasing N to form a continuum absorption band; this is said to occur involving only the nitrogen states without any explicit interaction with the host conduction band. The empirical pseudopotential model has been used to undertake detailed studies of the band structure of GaP_{1-x}N_x supercells, identifying both N-related localized states and also host states which are strongly perturbed due to the introduction of nitrogen. The two-level BAC model was originally introduced to describe the evolution of the lowest conduction band in GaAs_{1-x}N_x in terms of an interaction between the host Γ conduction band minimum and a higher-lying band of N resonant states.

The two-band BAC model provides a simplified view of the conduction band structure, making two major assumptions concerning the band structure. We show here how one of

those assumptions is reasonable when describing the optical properties of GaP_{1-x}N_x but that the second assumption needs modification and generalization to get a quantitative description of the lowest conduction states and their optical properties. Concerning the first assumption, the BAC model assumes that the chief effect of an isolated N atom is to introduce a single N-related defect state just below the X conduction band minimum of GaP. More complete calculations [4] show that when a single nitrogen atom is placed within a large supercell (up to 1728 atoms) it introduces numerous perturbed states, with Γ , X and L character, throughout the conduction band. However these calculations, and the tight-binding (TB) calculations which we present below, show that only a single N state in such a supercell has appreciable Γ character close to the X point energy. Because the valence band maximum is largely unperturbed due to the introduction of N, it is therefore reasonable to describe direct optical recombination in terms of transitions between the Γ -related N-induced state and the valence band maximum³. However the second assumption in the 2-level

³ Recent calculations [5] have shown that some L character is mixed into the valence states just below the valence band maximum, and that this mixing is important for optical transitions in the 2.5–3.2 eV range, for N concentrations above 1.5%. The present paper considers transitions at and below the GaP indirect gap of 2.35 eV, so that these valence L states can therefore be ignored in the analysis presented here.

BAC model is that all N atoms introduce a defect state at the same energy in $\text{GaP}_{1-x}\text{N}_x$. Both experiment [2] and detailed calculations [3–5] show that this is not the case. We find for instance using the TB method that when a single Ga atom has two N neighbours, this NN pair introduces a defect state at 2.180 eV, 126 meV below the calculated isolated N defect state energy. Interactions between N atoms which are near neighbours also leads to an inhomogeneous broadening of the defect state energy spectrum, while larger N clusters which form with increasing composition x also introduce defect energy levels deeper in the GaP gap. We have shown previously that this distribution of N state energies is crucial to understanding several of the properties of GaAsN alloys [11–16], and also of GaSbN and InSbN [17]. We show here that the distribution of N state energies is also key to understanding the lowest conduction states in $\text{GaP}_{1-x}\text{N}_x$.

We begin in section 2 by using an sp^3s^* TB Hamiltonian to investigate the evolution of the electronic structure of ordered $\text{GaP}_{1-x}\text{N}_x$ supercells with increasing N composition x . These ordered structures have just one N-related state with significant Γ character below the GaP conduction band minimum, and so are an ideal system to test the principles of the 2-level BAC model for GaPN structures. We analyse the TB results to show that the evolution of the lowest conduction band states in such ordered GaPN structures is indeed very well described by the 2-level BAC model. We then use the TB method in section 3 to investigate the electronic structure of 1000-atom disordered GaPN supercells. We find that average features of the electronic structure can still be described using the 2-level BAC model, including the total Γ character associated with the distribution of N levels, but that the 2-level BAC model omits much detail of the electronic structure.

We then show that the detail of the band structure of the 1000-atom supercells is well described by explicitly including the interactions between the different N levels and the GaP Γ conduction band minimum. Because N introduces such a strong perturbation, the results of the individual 1000-atom supercell calculations depend strongly on the distribution of the N atoms, including the number and relative positions of NN pairs and the presence or otherwise of larger and less common N clusters. We therefore probe the average conduction band properties of disordered $\text{GaP}_{1-x}\text{N}_x$ in section 4 by considering ultra-large supercells into which we typically place over 5000 randomly distributed N atoms, with the composition x determined by the size of supercell considered. The results of these calculations explain and are consistent with a wide variety of experimental observations, including systematic studies of electro-modulated absorption and photocurrent across a broad range of GaPN samples [18]. We conclude that the conduction band structure and optical transitions in $\text{GaP}_{1-x}\text{N}_x$ alloys are very well described by a modified BAC model which explicitly includes the interactions between the GaP Γ conduction band minimum and a linear combination of isolated but interacting N defect states.

2. Nitrogen states in ordered structures

The two-level BAC model explains the strong band gap bowing observed in $\text{GaAs}_{1-x}\text{N}_x$, where the energy gap decreases

rapidly, by over 100 meV per % of N for $x \leq 3\%$. This exceptionally large band gap reduction is explained in terms of an interaction between two levels, one at energy E_c associated with the extended conduction band edge states ψ_{c0} of the GaAs matrix, and the other at energy E_N associated with the higher-lying localized N impurity states ψ_{N0} , with the GaAsN conduction band minimum energy E_- then given by the lower eigenvalue [6]:

$$H = \begin{pmatrix} E_N & V_{Nc} \\ V_{Nc} & E_c \end{pmatrix} \quad (1)$$

where the interaction V_{Nc} between the quasi-localized N states and the GaAs conduction band minimum scales with N composition x as $V_{Nc} = \beta x^{1/2}$, with $\beta \sim 2.04$ eV in GaAsN [19], and where E_c and E_N in equation (1) can also depend on N composition x [19]. This 2-level BAC model accounts well for many features of GaAsN, including in particular the band gap bowing. However the single N level at energy E_N must be replaced by a distribution of N levels to explain e.g. the anomalously large electron effective mass values measured in many GaAsN samples [14, 20, 21], and also to account for the effective gyromagnetic factor [15] and intrinsically low mobility of electrons in GaAsN alloys [16, 22–25].

Turning to GaPN, the energy of the GaP Γ_{1c} conduction band minimum, E_c lies over 0.5 eV higher in energy than the N defect states. We expect in a 2-level BAC model that the lowest conduction levels in GaPN will therefore have predominantly N defect state character, ψ_{N0} , with just a small admixture of the GaP host Γ state, ψ_{c0} . We now use the TB method to explicitly evaluate the evolution of the lowest conduction state

$$\psi_- = \alpha_N \psi_{N0} + \alpha_c \psi_{c0} \quad (2)$$

in ordered GaPN supercells.

We do this by calculating and comparing the lowest conduction wavefunction ψ_- in a $\text{Ga}_L\text{P}_{L-1}\text{N}_1$ supercell with the Γ conduction band state ψ_{c0} of GaP [26]. We see from equation (2) that ψ_- is a linear combination of ψ_{c0} and ψ_{N0} , the wavefunction associated with an isolated N atom in an infinite GaP crystal. Knowing ψ_- and ψ_{c0} , we can therefore determine ψ_{N0} from equation (2) as $\psi_{N0} = (\psi_- - \alpha_c \psi_{c0}) / \sqrt{1 - \alpha_c^2}$ where $\alpha_c = \langle \psi_- | \psi_{c0} \rangle$. We can also then use ψ_{c0} , ψ_{N0} and the GaPN full TB Hamiltonian H to calculate $V_{Nc} = \langle \psi_{c0} | H | \psi_{N0} \rangle$, $E_N = \langle \psi_{N0} | H | \psi_{N0} \rangle$ and $E_c = \langle \psi_{c0} | H | \psi_{c0} \rangle$.

Calculating the probability density of the N defect state, $|\psi_{N0}|^2$, for each atom in the $\text{Ga}_{500}\text{P}_{499}\text{N}_1$ supercell shows that the N state is highly localized, with $\sim 5\%$ of its probability density on the N atom and $\sim 11\%$ on each of its 4 Ga neighbours. That is almost 50% of the probability density lying on these five central atoms. This is very similar to the localization of an isolated N resonant state calculated previously for $\text{GaAs}_{1-x}\text{N}_x$ [26].

Because the N state is so localized, we expect that we should be able to describe the lowest conduction states in ordered GaPN using the BAC model, as was the case for GaAsN [26]. To test this we have used the TB method to calculate the electronic structure of a series of

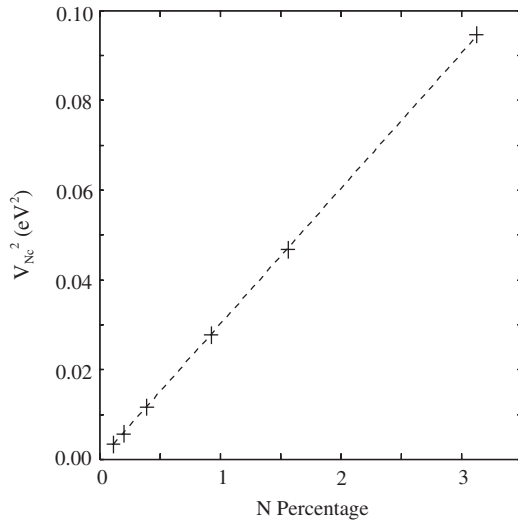


Figure 1. Calculated values of V_{Nc}^2 for a series of $\text{Ga}_L\text{P}_{L-1}\text{N}_1$ supercells. The straight line fit is obtained by assuming $V_{Nc}^2 = \beta^2 x$, with $\beta = 1.737$ eV.

ordered GaPN supercells. We considered ordered $\text{Ga}_L\text{P}_{L-1}\text{N}_1$ supercells containing 1728, 1000, 512, 216, 128 and 64 atoms respectively, with N composition ranging from 0.12% to 3.1%. The 128-atom supercell was made up of $4 \times 4 \times 4$ two-atom face-centred cubic unit cells, while the five other supercells were made up of $M \times M \times M$ eight-atom unit cells in a simple cubic arrangement with $2 \leq M \leq 6$. This limited number of ordered supercells were used to test the principle of the BAC model when all N atoms have an identical environment in GaPN.

Figure 1 shows the calculated values of $V_{Nc}^2 = |\langle \psi_{N0} | H | \psi_{c0} \rangle|^2$, plotted as a function of supercell nitrogen composition x . We show in figure 1 that V_{Nc}^2 varies almost linearly with x , as $\beta^2 x$, with the calculated values of β varying between 1.690 and 1.740 eV for the different structures considered. This calculated value of β for GaPN is considerably less than the values of 2.7 eV [9], 3.05 eV [7] and 4.38 eV [10] fitted by previous authors to experiment. We note however that the difference in electronegativity and in atom size between N and P atoms is less than that between N and As. This is consistent with the calculated value of β being less in GaP than in GaAs, because the interactions which contribute to β depend on the differences between the host material and N-related potential [27]. The experimentally derived values of β for GaPN were obtained by fitting to photoluminescence (PL) spectra in samples containing many N clusters, where the variation of PL energy with composition is most likely dominated by the evolution of deeper defect levels due to N clusters.

The Γ character, $|\langle \psi_- | \psi_{c0} \rangle|^2$, of the conduction band minimum plays a large role in determining the optical properties of the alloy, giving a direct indication of the probability for optical absorption and emission. The solid lines in figure 2 show the calculated energy spectrum $G_\Gamma(E)$ in the conduction band of the six ordered $\text{Ga}_L\text{P}_{L-1}\text{N}_1$ structures, projected onto the GaP Γ conduction band state, ψ_{c0}

$$G_\Gamma(E) = \sum |\langle \psi_i | \psi_{c0} \rangle|^2 \delta(E - E_i), \quad (3)$$

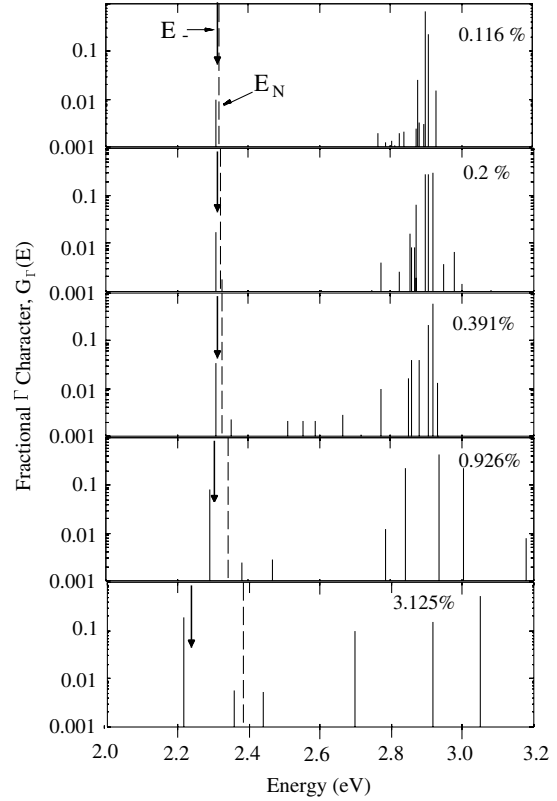


Figure 2. Γ character of the lowest conduction band states in ordered $\text{Ga}_L\text{P}_{L-1}\text{N}_1$ structures. The dashed line shows the value of $E_N = \langle \psi_N | H | \psi_N \rangle$ calculated for each structure. The y-axis is plotted on a log scale to show the emergence of the Γ character of E_- with increasing x . The vertical arrows show the value of E_- calculated for each structure using the 2-level BAC model of equation (1).

where E_i and ψ_i are the energy and wavefunction of the i th zone centre state in the GaPN supercell. The dashed lines show the value of E_N (calculated for each supercell from $E_N = \langle \psi_N | H | \psi_N \rangle$). We note that the calculated value of E_N varies with composition x , due to the interaction of N atoms in neighbouring unit cells with each other [26]. The E_- energy level can be clearly seen below the E_N level in each case, moving down in energy and increasing in Γ character for increasing N composition x . The vertical arrows in figure 2 shows the value of E_- determined for each structure using the calculated values of E_N and V_{Nc} for each supercell and using the calculated value of E_c in GaP. By solving the 2-level BAC model of equation (1), we expect the Γ character $|\alpha_c|^2$ of the E_- level to vary with N composition as

$$|\alpha_c|^2 = \frac{1}{2} \left(1 - \frac{1}{\sqrt{1 + y^2}} \right), \quad (4)$$

where $y^2 = 4\beta^2 x / (E_N - E_c)^2$.

Figure 3 compares the Γ character of the E_- state extracted directly from the TB calculations (pluses) with the predicted variation of Γ character from equation (4), calculated using the values of $E_N = 2.34$ eV, $E_c = 2.89$ eV and $\beta = 1.737$ eV (dashed line). We noted above that the values of E_N and E_c both vary with N composition x . We fix E_N

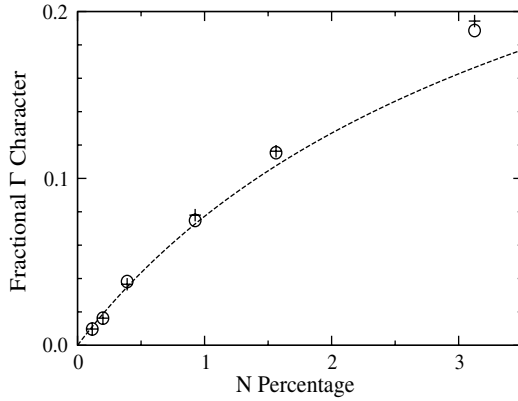


Figure 3. Γ character of the lowest conduction band state in ordered $\text{Ga}_L\text{P}_{L-1}\text{N}_1$ structures calculated using the TB method (pluses) and a BAC model (circles) where the parameters E_N and V_{Nc} are determined directly from the TB calculations. The dashed line is calculated using a 2-band BAC model with $E_N = 2.34$ eV, $E_c = 2.89$ eV and $\beta = 1.737$ eV. The discrepancy between the TB (pluses) and BAC (circles) results is due to neglecting the self-energy shift in E_c in the BAC calculation.

and E_c to their values for small x for the dotted curve in figure 3, while the circles show the calculated Γ character when we use the values of E_N from figure 2 in equation (4). We see that the observed evolution of Γ character is in good agreement with that predicted using the 2-band BAC model. Overall we conclude that the results presented in figures 1–3 confirm the validity of using the 2-level BAC model to describe the evolution of the lowest conduction state with increasing N composition x in ordered $\text{Ga}_L\text{P}_{L-1}\text{N}_1$ supercells.

3. N states in disordered structures

Having established that the BAC model describes well the lowest conduction states in ordered $\text{Ga}_L\text{P}_{L-1}\text{N}_1$ structures, we now use the TB method to examine the band structure of disordered GaPN, considering 1000-atom supercells with up to 5% N atoms placed at random on the group V sites (i.e. up to 25 N atoms per supercell).

Figure 4 shows the calculated energy of the lowest N-related conduction state for a series of such structures with increasing N composition, along with the predicted variation of band edge energy with x , using the 2-level BAC model of the previous section, with $\beta = 1.737$ eV, $E_N = 2.34$ eV and $E_c = 2.89$ eV. The BAC model gives reasonable agreement with the individual TB calculations of the 1000-atom supercells for structures in which the individual N atoms are largely independent of one another. However the calculated energy of the lowest conduction state drops significantly below the BAC value in one of the structures for $x = 2\%$ and in all other structures for higher x . This is because the 1000-atom supercells at these higher compositions contain e.g. N pairs, where a single Ga atom has two N neighbours, and also larger N clusters. The calculated conduction band minimum energy then starts to vary significantly between different calculations at larger x , because of larger differences in the detail of the N arrangements in the different 1000-atom supercell calculations.

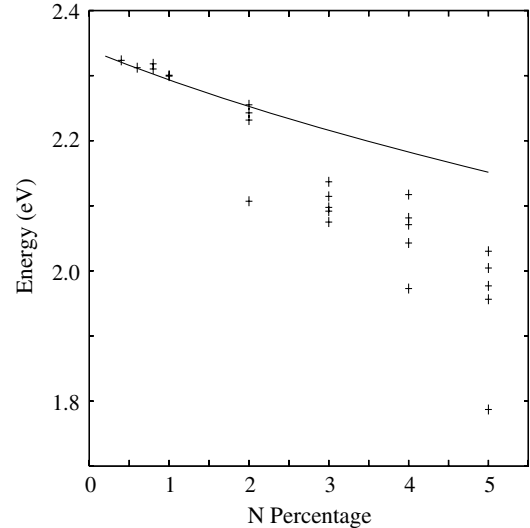


Figure 4. Comparison of the lowest N-related conduction state energy calculated using the BAC model (line) with the energy obtained from individual 1000-atom supercell TB calculations (pluses).

We saw previously for $\text{Ga}_{500}\text{As}_{500-M}\text{N}_M$ supercells that the energy and wavefunction of the conduction band edge (CBE) state can be well represented by the interactions between the GaAs CBE wavefunction, ψ_{c0} , and a linear combination of M isolated N states (LCINS method) [11, 12], where the LCINS model includes not only the energy levels and wavefunctions of isolated N atoms but also of NN pairs and other N clusters [11, 14, 22]. We show here that we can likewise associate a localized defect state ψ_{Ni} with each of the M nitrogen atoms in a $\text{Ga}_{500}\text{P}_{500-M}\text{N}_M$ supercell ($i = 1, \dots, M$). Using the LCINS method, we can then analyse the supercell conduction band states by solving the $(M+1) \times (M+1)$ matrix equation linking the M defect states with each other and with the unperturbed GaP Γ conduction band minimum, ψ_{c0} . We have

$$H_{ij}\phi_j = ES_{ij}\phi_j, \quad (5)$$

where $H_{ij} = \langle \psi_{Ni} | H | \psi_{Nj} \rangle$ and $H_{i,M+1} = \langle \psi_{Ni} | H | \psi_{c0} \rangle$, $1 \leq i, j \leq M$, with H the full GaPN Hamiltonian, and $S_{ij} = \langle \psi_{Ni} | \psi_{Nj} \rangle$ a matrix reflecting that neighbouring N states can overlap each other.

The upper panels in figure 5 (labelled (a)) show $G_\Gamma(E)$, the Γ character (calculated using the TB method) for a representative set of random $\text{GaP}_{1-x}\text{N}_x$ 1000-atom supercells. We see that as the N concentration increases, the Γ character tends to be distributed over more than one N-related low energy level. The distribution of the Γ character depends strongly on the local N environment in the 1000-atom supercells. The lower panels (labelled (b)) show $G_\Gamma(E)$ calculated using the LCINS method described above, where we explicitly treat the interaction between the GaP Γ CBE and the same random distribution of N defect states. We see good agreement between the LCINS and full TB calculations in figure 5 for the lowest conduction band states in the disordered GaPN supercells considered. Because the 2-level BAC and LCINS models include only one host Γ conduction band state, ψ_{c0} ,

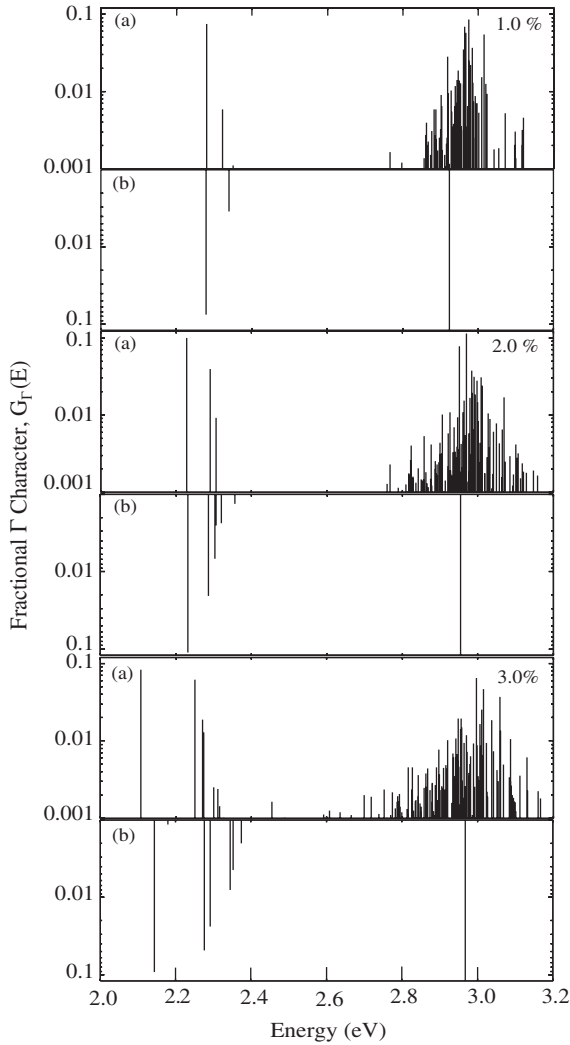


Figure 5. Fractional Γ character of the lowest conduction band states in three 1000-atom supercells containing a random distribution of N atoms. The Γ character of each state is plotted on a log scale and was calculated (a) using the full tight-binding method, and (b) using the LCINS method.

they predict the formation of a single higher-lying energy level, referred to as E_+ , above the GaP Γ level at 2.89 eV in figure 5(b). In practice, the GaP Γ level is degenerate with a large density of other conduction states. The E_+ level hybridizes with many of these other conduction levels, as observed in the full TB calculations of figure 5(a). This hybridization was also observed when comparing LCINS and TB calculations of $\text{GaAs}_{1-x}\text{N}_x$ alloys [28]. The LCINS model cannot reproduce this hybridization, because it only includes a single GaP host conduction band state. Therefore the distribution of energy levels in the vicinity of the host Γ conduction band (seen in the TB calculation) are represented by this single level. However, the good agreement between the LCINS and full TB calculations for the low energy states in figure 5 confirm the validity of this modified BAC model to describe the lowest conduction states in a disordered GaPN supercell. The calculated increase in E_+ energy is also in agreement with the results of photoreflectance

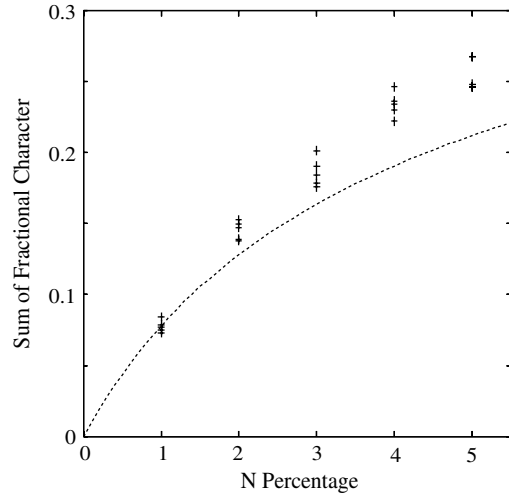


Figure 6. Total Γ character summed over the lowest conduction levels for a series of TB calculations (pluses), compared with the predicted variation of Γ character with composition, using the 2-level BAC model with $E_N = 2.34$ eV, $E_c = 2.89$ eV and $\beta = 1.737$ eV (dashed line).

measurements, which show a broadening and upward shift of E_+ with increasing N composition x [18].

Although the Γ character is distributed over several N levels near the conduction band minimum in figure 5, we could still expect the total Γ character integrated over these N levels to be well described by the 2-level BAC model in a random GaPN supercell. Figure 6 confirms that this is the case for low N composition. From figure 6 it can be seen that there is good agreement between the predicted and calculated Γ character for low N composition, but that the 2-level BAC model with fixed E_N , E_c and V_{Nc} starts to underestimate the total character at larger x , in a similar way to what was previously observed in figure 3.

In summary, the BAC model predicts that the total Γ character, f_Γ mixed into the lowest conduction band states increases with N composition x , from $f_\Gamma \sim 7.7\%$ for 1% N up to 12.7% for 2% N in the case of a single nitrogen-induced level (i.e. in the ordered structures of section 2). The TB model predicts a very similar total Γ character associated with the N-induced levels in a disordered structure, but the distribution of this Γ character depends upon the distribution of N atoms within the supercell. Comparing the BAC and TB models, the Γ character of the E_- state in the 2-level BAC model is close to the total Γ character integrated over the nitrogen states near to the band edge in the full TB calculation. As the N concentration is increased, the probability of forming nearest neighbour N pairs, second neighbour N pairs, and larger N complexes increases rapidly. The 2-level BAC model ignores these N complexes, whose energy and Γ character are inherently accounted for using the TB method. In the TB calculations, the Γ character remains reasonably constant with respect to N concentration (see figure 6), but is distributed over the N levels depending on the local N configurations within the supercell (figure 5). The local nitrogen configuration therefore plays a key role in understanding the band structure of $\text{GaP}_{1-x}\text{N}_x$.

Because N introduces such a strong perturbation, we see from figures 4–6 that the results of an individual 1000-atom supercell calculation depend strongly on the distribution of N atoms within the supercell. We therefore need to choose significantly larger supercells in order to minimize the effects of different random distributions of N atoms. We estimate that these supercells should contain at least 5000 N atoms [11], with the composition x determined by the size of the supercell considered (e.g. $x = 1\%$ for a 1000000-atom supercell containing 5000 N atoms). We cannot use the TB method to directly calculate the electronic structure of such a large supercell. We see however from figure 5 and other calculations we have undertaken [11, 12, 22] that the LCINS model describes well the electronic structure of the lowest conduction states in dilute nitride alloys. We therefore extend the LCINS model in the next section to investigate the lowest conduction states in ultra-large disordered $\text{GaP}_{1-x}\text{N}_x$ supercells.

4. N states in ultra-large disordered $\text{GaP}_{1-x}\text{N}_x$ supercells

The LCINS approach models the interaction of the N states with the host (unperturbed) Γ conduction band minimum, while also incorporating the complexities of the local N environment. We treat ultra-large supercells containing $M \sim 5000$ nitrogen atoms, with the N atoms being placed at random on the Group V sites in the lattice. The composition x is then determined by the size of the supercell. We start here by first examining the evolution of both the nitrogen density of states and their Γ character for N concentrations less than 1%.

We first consider the distribution of N cluster state energies, by diagonalizing the $M \times M$ matrix linking the M individual N states ψ_{Ni} to get M nitrogen cluster states ψ_{NI} with energies ϵ_i . We can then evaluate the interactions $V_{Ni} = \langle \psi_{Ni} | H | \psi_{c0} \rangle$ between these cluster states and the unperturbed GaP Γ conduction band minimum state, ψ_{c0} . The histograms in figure 7 show the evolution of the distribution of N cluster state energies, ϵ_i , weighted by their interaction with the GaP Γ CBE, as x increases from 0.008% to 1.0%, where we plot in each case $V_N(E) = \sum V_{Ni}^2 T(E - \epsilon_i)$, and where $T(x)$ is a top-hat function of width 2 meV and unit area [11]. For very low N composition (e.g. $x = 0.05\%$), most of the interaction arises from states which lie close to the isolated N defect level ($E_N = 2.306$ eV). A small feature due to NN(110) pairs is observed about 2.180 eV for $x = 0.2\%$, as well as another weak feature at 2.282 eV, due to NN(220) pairs, where we have two N atoms on opposite corners of a FCC unit cell face. A further feature is found at 2.298 eV associated with NN(211) pairs. These assignments are made by examining the wavefunctions of the states and comparing these with calculations carried out on a supercell containing just a single (110), (200) or (211) pair. It can be seen that the number of pair states increases rapidly with increasing x (approximately as x^2), and that the different peaks are also inhomogeneously broadened with increasing x , due to interactions with an increasing number of more distant N atoms.

Low-temperature photoluminescence (PL) measurements [2] on a $\text{GaP}_{1-x}\text{N}_x$ sample with $x = 0.05\%$ show a broadly

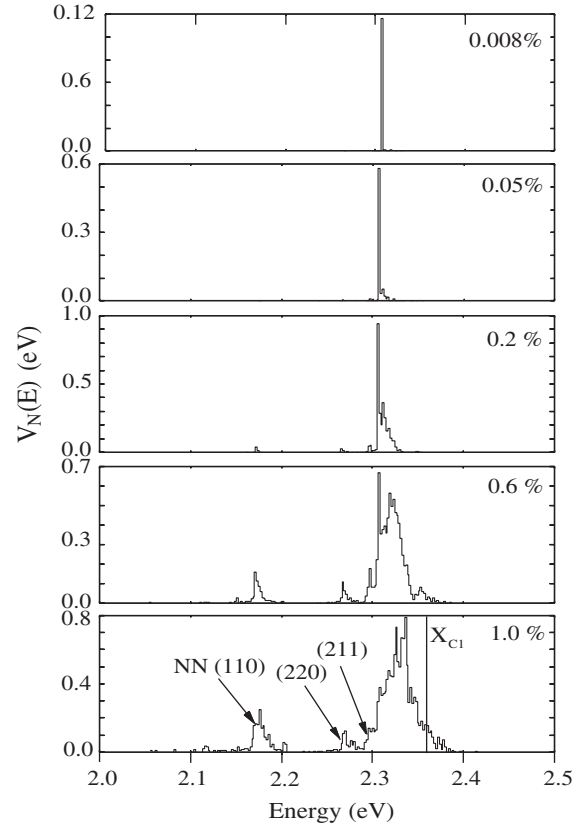


Figure 7. Evolution of the nitrogen state energies weighted by the square of their interaction with the Γ conduction band minimum for 0.008% N to 1.0% N, calculated using the LCINS model. The emergence of energy states due to 1st nearest neighbour NN(110) pairs as well as (220) and (211) pairs is clearly seen with increasing N concentration. The GaP X point energy (X_{C1}) is shown for reference in the lowest panel (1.0% N case).

similar distribution of peak energies compared to the energy levels presented in figure 7, with low energy peaks (labelled NN_1 and NN_3) at 2.188 and 2.266 eV, close to the calculated NN(110) and (220) levels, and then a gap of about 25 meV to a series of further peaks (NN_4 to NN_8) between 2.291 eV and 2.311 eV, the energy range in which the NN(211) pair and isolated N level are both calculated to occur.

Figure 8 shows $G_\Gamma(E)$ for the N state distributions of figure 7, calculated by diagonalizing the $(M + 1) \times (M + 1)$ Hamiltonian matrix $H_{ij}\phi_j = ES_{ij}\phi_j$ of equation (5). We see for low N composition ($x \leq 0.05\%$ here) that the interaction between the GaP Γ CBE and the isolated N defect levels leads to a E_- -like level almost degenerate with the isolated N energy level (labelled E_N in figure 8). However the form of the calculated Γ spectrum, $G_\Gamma(E)$, changes significantly at higher N composition. We see at higher x that the Γ character is now distributed over bands of N states, where many LCINS states each acquire a small Γ character, with the Γ character appearing predominantly on the low energy side of the different bands of levels plotted in figure 7. Three main peaks are observed by $x = 1\%$, one centred at 2.173 eV, just below the NN(110) isolated energy levels and two more at 2.262 and 2.287 eV, close to the NN(220) and (211) levels.

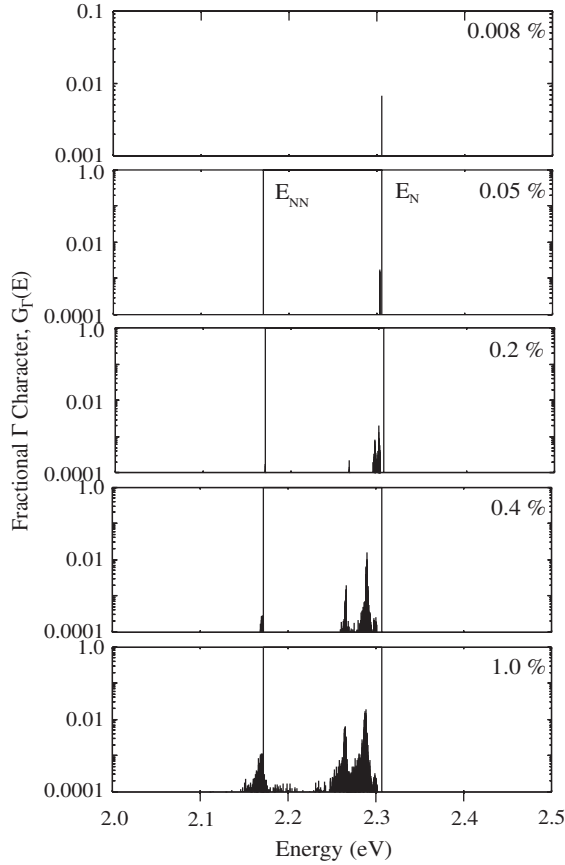


Figure 8. The evolution of $G_{\Gamma}(E)$, the projection of the LCINS spectrum onto the unperturbed GaP Γ conduction band minimum state for 0.008% N to 1.0% N. The lines E_N and E_{NN} show the positions of the isolated N state energy and the NN(110) pair state energy respectively. The y-axis is plotted on a log scale to show more clearly the distribution of Γ character. Note that the top panel ($x = 0.008\%$) has a different y scale than the other panels.

Little downward shift of these N-related energy levels is observed compared to what we would expect based on the 2-level BAC model, and compared also to the downward shift observed for E_- in the ordered $\text{GaP}_{1-x}\text{N}_x$ structures in section 2. This marked change can be understood by comparing the analytical solution of the 2-level BAC model of equation (1) with the results of diagonalizing the large LCINS matrices considered here.

The sum of the eigenvalues of equation (1) equals the sum of the diagonal matrix elements

$$E_+ + E_- = E_N + E_c \quad (6)$$

so that the single lower eigenvalue, E_- of the 2×2 matrix of equation (1) then becomes shifted down by as large an energy as the upper eigenvalue E_+ is shifted upwards.

The upper level E_+ experiences a similar upwards energy shift in the LCINS and 2-level BAC models. Therefore, the sum of all the lower N eigenvalues will be shifted downward in the LCINS model by a similar magnitude as E_+ is shifted upwards. This downwards shift is however spread over many energy levels in the LCINS model, so that each individual energy level therefore experiences a much smaller

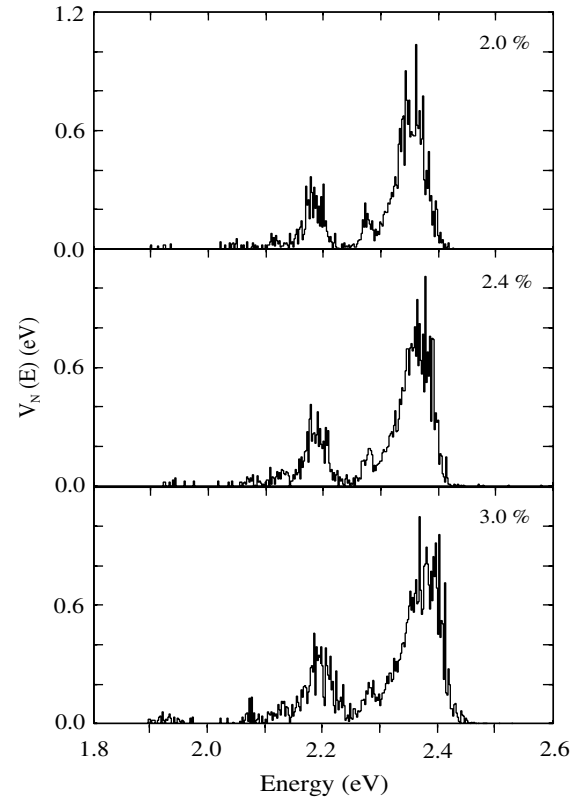


Figure 9. Evolution of the nitrogen state energies weighted by the square of their interaction with the Γ conduction band minimum calculated using the LCINS model, as the N composition is increased from 2.0% to 3.0% N.

downwards shift than predicted by the 2-level BAC model. This reduced shift in the LCINS model is consistent with careful experimental measurements of the band edge shift with increasing N composition x in $\text{GaP}_{1-x}\text{N}_x$ samples with very low x , where little shift is observed in the lowest Γ -related CBE states up to $x \sim 0.1\%$ [1]. We see from figure 7 that an increasing number of lower energy N states start to appear above $x \sim 0.2\%$, including NN(110), (220) and (211) pair states. This increasing density of lower energy states then interacts with the higher-lying GaP Γ conduction band minimum, leading to an increasing density of optically active Γ related states at lower energies, as presented in figure 8.

The Γ character in figure 8 is in each case spread over many N-related levels, but the total Γ character summed over all the N states is close to the total Γ character predicted by the full TB and by the 2-level BAC model at each composition. For example, the total Γ character integrated over the LCINS states is 7.7% for a nitrogen composition of 1%, compared with a predicted Γ character of 7.7% from the 2-level BAC model. The occurrence of several sharp Γ -related features in figure 8 is also consistent with the observed evolution of the electro-modulated absorption spectrum in $\text{GaP}_{1-x}\text{N}_x$ [18].

Figure 9 shows the calculated evolution of N-related cluster state energies for higher N concentrations (i.e. 2%–3%). We note that there is a further increase in the inhomogeneous broadening of the state distribution, and in the number of NN(110) states, while we also start to see the evolution of

lower energy states, due to larger N clusters. Figure 10 shows the calculated evolution of the Γ character, $G_{\Gamma}(E)$, including a continued down-shift in the Γ character towards the lower edges of the cluster peaks, but still showing a broad energy distribution for the total Γ character. The Γ character shifts more strongly to the nearest neighbour NN(110) pair states, with increasing Γ character also found on the lowest energy states associated with larger N clusters. This leads to a quasi-continuous downward shift of the lowest Γ related states with increasing x . This downwards shift has been modelled by previous authors using the 2-level BAC model [7, 9, 10]. The LCINS results presented here suggest that the reported agreement between the 2-level BAC model and experiment for GaPN is in large part fortuitous: whereas the BAC model assumes that the lowest GaP Γ conduction band state effectively interacts with and repels a single N-related level with a well-defined energy, we see here that the GaP Γ state interacts and mixes with many N-related levels. The energy of each N-related state is shifted very little through its interaction with the Γ level, but the distribution of these levels varies with x , with an increasing number of lower energy states emerging as x is increased.

5. Conclusion

In conclusion, we have carried out a detailed analysis of the evolution of the lowest conduction band levels in $\text{GaP}_{1-x}\text{N}_x$ as the N composition x is increased up to $x \sim 3\%$.

Tight-binding (TB) calculations of $\text{Ga}_L\text{P}_{L-1}\text{N}_1$ supercells show that the lowest conduction level in ordered structures is well described by a 2-level band-anti-crossing (BAC) model [6], which describes the evolution of the band structure in terms of an interaction between the GaP host Γ conduction band minimum and an isolated localized N defect level, which lies just below the X conduction band minimum of GaP. The N defect level is highly localized and very similar in character to the N resonant state in GaAsN [12]. The BAC interaction accounts well both for the downward shift of the lowest conduction level and its increasing Γ character with increasing N composition in ordered GaPN structures.

When we introduce a random distribution of M N atoms to form a $\text{Ga}_L\text{P}_{L-M}\text{N}_M$ supercell, we find a distribution of N-related defect levels below the X conduction band minimum of GaP, in good agreement with experiment. This distribution of N-related levels is crucial to understanding the electronic and optical properties of GaPN alloys. The TB calculations show a very similar value for the total Γ character mixed into the N levels in the ordered and disordered cases but a wider distribution of states with Γ character in the disordered case. This mixing of Γ character across a range of levels can then account for the broad PL emission spectra observed experimentally in GaPN alloys.

Because N introduces such a strong perturbation, the results of individual TB calculations on 1000-atom supercells depend strongly on the distribution of N atoms in the supercell, including the number of NN pairs and the occurrence of larger and less common N clusters. We therefore introduced a modified BAC model, which we refer to as

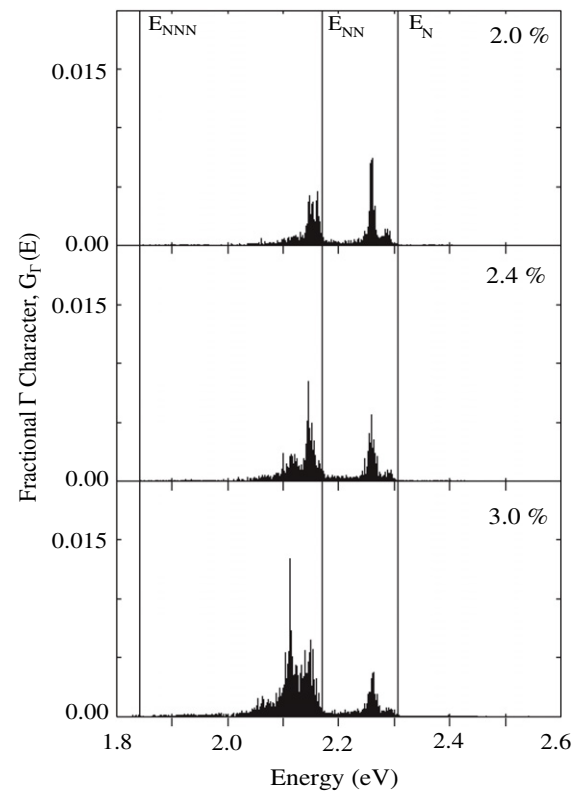


Figure 10. The evolution of $G_{\Gamma}(E)$, the projection of the LCINS spectrum onto the unperturbed GaP Γ conduction band minimum state for 2.0% to 3.0% N. The lines E_N , E_{NN} and E_{NNN} show the positions of the isolated N state energy, the NN(110) pair state energy and the NNN triple state energy respectively.

the LCINS method [11], to describe ultra-large supercells, where we explicitly treat the interactions between the GaP Γ conduction band minimum and a linear combination of randomly distributed nitrogen atoms. This model reproduced well the results of 1000-atom TB calculations but also allowed us to minimize the effects of statistical fluctuations in the N distribution. Because the Γ level interacts with many different N states in the LCINS model, no one N level experiences a strong downward shift in energy, contrary to the prediction of the 2-level BAC model. Instead Γ character is distributed across several bands of N levels which emerge with increasing N composition.

Overall, the results of the LCINS calculations explain and are consistent with a wide variety of experimental observations. We conclude that the conduction band structure and optical transitions in $\text{GaP}_{1-x}\text{N}_x$ alloys are therefore very well described by such a modified BAC model, which explicitly includes the broad distribution of N levels in disordered GaPN alloys.

Acknowledgments

This work was supported by Science Foundation Ireland. We thank P J Klar and M Güngerich for useful discussions, and for details of unpublished experimental measurements.

References

- [1] Fluegel B, Zhang Y, Geisz J F and Mascarenhas A 2005 *Phys. Rev. B* **72** 073203
- [2] Zhang Y, Fluegel B, Mascarenhas A, Xin H P and Tu C W 2000 *Phys. Rev. B* **62** 4493
- [3] Kent P R C and Zunger A 2001 *Phys. Rev. B* **64** 115208
- [4] Dudiy S V, Kent P R C and Zunger A 2004 *Phys. Rev. B* **70** 161304
- [5] Dudiy S V, Zunger A, Felici M, Polimeni A, Capizzi M, Xin H P and Tu C W 2006 *Phys. Rev. B* **74** 155303
- [6] Shan W, Walukiewicz W, Ager J W III, Haller E E, Geisz J F, Friedman D J, Olson J M and Kurtz S R 1999 *Phys. Rev. Lett.* **82** 1221
- [7] Shan W, Walukiewicz W, Yu K M, Wu J, Ager J W III, Xin H P and Tu C W 2000 *Appl. Phys. Lett.* **76** 3251
- [8] Wu J, Walukiewicz W, Yu K M, Ager J W III, Haller E E, Hong Y G, Xin H P and Tu C W 2002 *Phys. Rev. B* **65** 241303
- [9] Buyanova I A, Izadifard M, Chen W M, Xin H P and Tu C W 2004 *Phys. Rev. B* **69** 201303
- [10] Chamings J, Ahmed S, Sweeney S J, Odnoblyudov V A and Tu C W 2008 *Appl. Phys. Lett.* **92** 021101
- [11] Lindsay A and O'Reilly E P 2004 *Phys. Rev. Lett.* **93** 196402
- [12] O'Reilly E P, Lindsay A and Fahy S 2004 *J. Phys.: Condens. Matter* **16** S3257
- [13] Patanè A, Endicott J, Ibañez J, Brunkov P N, Eaves L, Healy S B, Lindsay A, O'Reilly E P and Hopkinson M 2005 *Phys. Rev. B* **71** 195307
- [14] Masia F, Pettinari G, Polimeni A, Felici M, Miriametro A, Capizzi M, Lindsay A, Healy S B, O'Reilly E P, Cristofoli A, Bais G, Piccin M, Rubini S, Martelli F, Franciosi A, Klar P J, Volz K and Stolz W 2006 *Phys. Rev. B* **73** 073201
- [15] Pettinari G, Masia F, Polimeni A, Felici M, Frova A, Capizzi M, Lindsay A, O'Reilly E P, Klar P J and Stolz W 2006 *Phys. Rev. B* **74** 245202
- [16] Fahy S, Lindsay A, Ouerdane H and O'Reilly E P 2006 *Phys. Rev. B* **74** 035203
- [17] Lindsay A, O'Reilly E P, Andreev A D and Ashley T 2008 *Phys. Rev. B* **77** 165205
- [18] Güngerich M, Klar P J, Heimbrodt W, Weiser G, Geisz J F, Harris C, Lindsay A and O'Reilly E P 2006 *Phys. Rev. B* **74** 241202(R)
- [19] Lindsay A and O'Reilly E P 1999 *Solid State Commun.* **112** 443
- [20] Hai P N, Chen W M, Buyanova I A, Xin H P and Tu C W 2000 *Appl. Phys. Lett.* **77** 1843
- [21] Masia F, Polimeni A, Baldassarri G, Von Hogerthal Hoger, Bissiri M, Capizzi M, Klar P J and Stolz W 2003 *Appl. Phys. Lett.* **82** 4474
- [22] Polimeni A, Masia F, Pettinari G, Trotta R, Felici M, Capizzi M, Lindsay A, O'Reilly E P, Niebling T, Stolz W and Klar P J 2008 *Phys. Rev. B* **77** 155213
- [23] Geisz J F and Friedman D J 2002 *Semicond. Sci. Technol.* **17** 769
- [24] Skierbiszewski C 2002 *Semicond. Sci. Technol.* **17** 803
- [25] Fahy S and O'Reilly E P 2003 *Appl. Phys. Lett.* **83** 3731
- [26] Lindsay A and O'Reilly E P 2001 *Solid State Commun.* **118** 313
- [27] Lindsay A and O'Reilly E P 2003 *Physica B* **340** 434
- [28] Lindsay A and O'Reilly E P 2004 *Physica E* **21** 901